A practical gait feedback method based on wearable inertial sensors for a drop foot assistance device

Lin Meng, Uriel Martinez-Hernandez, Craig Childs, Abbas A. Dehghani-Sanij and Arjan Buis

***Abstract*—To maximise the efficiency of gait interventions, gait phase and joint kinematics are important for closing the system loop of adaptive robotic control. However, few studies have applied an inertial sensor system including both gait phase detection and joint kinematic measurement. Many algorithms for joint measurement require careful alignment of the inertial measurement unit (IMU) to the body segment. In this paper, we propose a practical gait feedback method, which provides sufficient feedback without requiring precise alignment of the IMUs. The method incorporates a two-layer model to realise simultaneous gait stance and swing phase detection and ankle joint angle measurement. Recognition of gait phases is performed by a high-level probabilistic method using angular rate from the sensor attached to the shank while the ankle angle is calculated using a data fusion algorithm based on the complementary filter and sensor-to-segment calibration. The online performance of the algorithm was experimentally validated when 10 able-bodied participants walked on the treadmill with three different speeds. The outputs were compared to the ones measured by an optical motion analysis system. The results showed that the IMU-based algorithm achieved a good accuracy of the gait phase recognition (above 95%) with a short delay response below 20 ms and accurate angle measurements with root mean square errors below 3.5° compared to the optical reference. It demonstrates that our method can be used to provide gait feedback for the correction of drop foot.**

***Index Terms*—inertial measurement units, gait analysis, gyroscopes and accelerometers, gait phase recognition, ankle angle measurement, hierarchical structure, sensor data fusion**

I. Introduction

STROKE, brain injury, spinal cord injury and other neurological diseases usually result in locomotion deficits, such as drop foot gait. An individual with a drop foot suffers from a limited ability to lift the foot during early swing phase. It would lead to a pathological gait with a high risk of tripping and falling and have a negative impact on the persons' independence to perform activities of daily living [1], which would influence their quality of life. A drop foot assist device is usually a wearable medical device that is attached to the wearer's ankle and foot, aiming to provide a certain amount of actuation for the correction of drop foot. To maximise the efficiency of gait interventions, real-time information presenting the ankle-foot movement need to be explored to augment proprioceptive inputs synchronised with gait cycles [2], [3].

The powered ankle devices have been actively researched in recent decades. Park et al. [4] developed a wearable soft robotic device that provides active assistance for use in ankle-foot rehabilitation. A novel compliant knee-ankle-foot orthosis developed by Patane et al. [5] was controlled based on the gait phase recognition and the regulation of the equilibrium of series elastic actuators. Zhang et al. [6] constructed an ankle rehabilitation robot for treating drop foot associated with neuromuscular disorders by controlling the joint trajectories.

Most devices for drop foot correction depend on simple and fixed pattern control where gait events switch on/off the external assistance, making these robots susceptible to failure during the assistance to human [7]. These systems realise the automatic identification of gait events using various sensors, such as foot pressure insoles, foot switches, inertial measurement units (IMUs), electromyography (EMG) signals and etc. A simple approach involving foot switches or force sensitive resistors (FSRs) to detect the foot contact provided satisfactory results for healthy subjects. However, foot contact sensors cannot provide any information during the swing phase and the sensor reliability reduces when subjects have drop foot or shuffling gait [8], [9]. A combination of the inertial sensors and foot sensors (such as foot switch, FSRs-embedded insole) increased the number of gait phases as the IMUs provide sufficient information correlated to locomotion, especially for the swing phase [8]. The IMUs have been popularly adopted in ambulatory systems due to their small size, low cost, and low power consumption. The use of either whole IMU consisting of gyroscopes, accelerometers, and magnetometers or parts of it to determine kinematic data [10], activity recognition [11] or gait event classification [12], [13] has shown promising results.

A robust human-machine interaction is of importance for the development of assistive devices used for daily living assistance. Real-time modulation requires sensory system providing the feedback for closing the loop in a robot controller [1], [14]. Human kinematics is thus important for advanced control of wearable robotics. However, few studies have applied an inertial sensor system for both gait phase detection and kinematic measurement. This study firstly aimed to develop a robust gait feedback method using a minimal number of sensors for both joint angle measurement and gait phase detection during

Manuscript submitted in April 2019. This work was supported by the Engineering and Physical Sciences Research Council (EPSRC) for the 'Wearable soft robotics for independent living' project (EP/M026388/1).

Lin Meng is with Tianjin International Joint Research Center for Neural Engineering, Academy of Medical Engineering and Translational Medicine, Tianjin University, Tianjin, China. (email: linmeng@tju.edu.cn)

Craig Childs and Arjan Buis are with the Department of Biomedical Engineering, University of Strathclyde, Glasgow, G1 1XQ, U.K. (email: craig.childs, arjan.buis@strath.ac.uk)

U. Martinez-Hernandez is with the Department of Electronic and Electrical Engineering, Faculty of Engineering and Design, University of Bath, Bath, BA2 7AY, U.K. (email: u.martinez@bath.ac.uk)

Abbas A. Dehghani-Sanij is with the Institute of Design, Robotics and Optimisation (iDRO), the School of Mechanical Engineering at the University of Leeds, Leeds, LS2 9JT, U.K. (email: mnsf, a.a.dehghani-sanij@leeds.ac.uk)

walking.

The rest of this paper is organised as follows: the related work is presented in Section II. The proposed method is presented in Section III.The experiments and results are described in Section IV. The discussion and conclusions are given in Section V and VI.

II. Related Work

Machine learning offers sophisticated algorithms for developing robust and adaptable systems for gait recognition. Artificial neural networks (ANN), fuzzy logic (FL) and hidden Markov models (HMM) were often used in the detection of gait phases [12], [15], [16], [17]. Williamson et al. [15] applied an adaptive logic network to a cluster of accelerometers attached to the shank for gait phases recognition. Taborri et al. [17] proposed a weighted HMM classifier that realised gait phases recognition utilising angular rates of the foot, shank, and thigh. The results of the decision index demonstrated that the thigh sensor never took the decision in the weighted algorithm whilst the combination of foot and shank sensors provided the best performance. Most methods require a network of sensors and produce black box models, making data synchronisation and collection and real-time implementation a complicated process. Probabilistic approaches provide well-defined mathematical models to develop reliable systems for perception. Yuwono et al.[18] presented a single IMU system that identifies bilateral heel-strike events with the use of the Bayesian method. Martinez-Hernandez et al. [11] proposed a Bayesian formulation to achieve high recognition accuracy of simultaneous daily activities and gait phases recognition with a small number of sensors.

A key problem on the measurement of joint angles using inertial sensors is drift resulted in error accumulation after time integration. Several methods have been proposed to eliminate the drift: strap-down method [19], [20], high-pass filtering [21]. Morris et al. [19] set the signal equal at the begin and end of every gait cycle. Sabatini et al. [20] proposed a method that calculates body segment orientation from the angular rate data and compensates the drift with the cycle properties. Tong et al. [21] derived the knee angle from segment angular velocities and applied a low-cut high-pass filter to remove the low-frequency component. Sensor fusion method seems a promising solution for the drift problem. The methods, such as Kalman filter [22] and complementary filter [10], [23], could correct offset drift at every time instant. Sensor orientations can be presented as quaternions calculated from 9D IMU data and the joint angle is derived from the relative orientation of two adjacent segments [24], [25]. However, the use of magnetometer measurement where magnetometer disturbances occur may limit the algorithm accuracy and its indoor application. An extended Kalman filter based segment orientation estimation methods via ground contact estimation was used to build a 3D joint kinematic model while omitting magnetometer data [26]. Laidig et al. [27] explored a quaternion-based method of exploiting kinematic constraints to compensate orientation error caused by magnetic disturbances. Favre et al. [28] proposed to use acceleration data to compensate the drift from the gyroscope-based angle. The complementary filter is relatively simple and easy to be applied in real-time applications. The sensor fusion of gyroscope-based and accelerometer-based angles has shown its good performance in gait analysis [10], [23].

The definition of human joint angle is based on the International Society of Biomechanics (ISB) recommendations [29]. Due to the complexity of human joint anatomy, inertial sensor-to-segment calibration is required to align IMU local axes with the joint axes. The current state of art approaches in sensor-to-segment calibration can be divided into three main types. Firstly, sensors are mounted with a predefined orientation towards the segment or joint. However, this is hard to realise for some applications, e.g. gait analysis, and sensor casings rarely coincide with inner coordinate systems, which may yield results with lower accuracy [30]. An alternative method is to estimate the local joint axes from predefined calibration motions [31]. Its accuracy relies upon the performance of the movements. Sensor-to-segment identification approaches have been proposed to determine the local joint axes and position coordinates by exploring the kinematics of the joint from arbitrary motions [10], [32], [33]. The automatic calibration approaches does not require precise placement of sensors attached to the body making the system more robust and practical for wearable applications.

For closing the loop of robotic control in drop foot assistance, this work proposed a new algorithm consisting of a hierarchical model. The high-level layer of the model realises the recognition of stance and swing phases with the use of a probabilistic method. The low-level calculates the ankle plantar-/dorsiflexion angle based on the data fusion of acceleration and angular rate whilst the joint axes are identified in the sensor-to segment calibration procedure. The details of the method are described in Section III.

III. Methods

Fig. 1A shows the structure of the system model consists of two layers. Two IMU sensors are attached to the shank and foot respectively while linear acceleration (a_i) and angular rate (ω_i) data are collected. Gait stance/swing phases are detected in the high-level layer with a Bayesian algorithm whilst the ankle dorsi-/plantarflexion angle is calculated in the low-level model.

A. High level - gait phase recognition

Recognition of gait phases is performed with a Bayesian formulation together with a sequential analysis method as shown in Fig. 1B. This probabilistic approach iteratively accumulates sensor data, reducing the uncertainty from sensors measurements. The sequential analysis method, which uses a belief threshold parameter, allows the recognition method to decide whether the information accumulated is enough to make a decision.

1) Bayesian update: The Bayesian method updates the posterior probability by multiplying the prior and likelihood distributions. Sensor measurements and classes are represented by ω and c_n, where n is the gait phase; stance or swing phase,

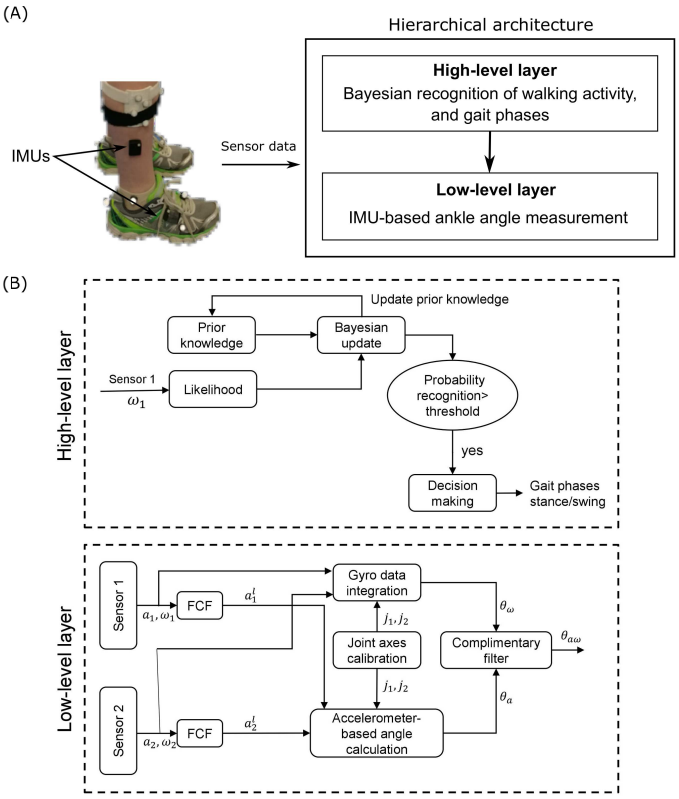

Fig. 1. (A) The gait measurement system has a hierarchical architecture model that consists of two layers. The high-level layer used Bayesian recognition algorithm to detect gait phases, and the low-level calculate measured the ankle plantar/dorsiflexion angle from acceleration and angular rate data. (B) The flow chart of the hierarchical architecture model. The high-level layer implements the Bayesian update based on the combination of prior knowledge and the likelihood. The algorithm evaluates the probability at each time instant in order to make a decision when the probability reaches the set-up threshold. The low-level layer uses a complementary filter to remove the angle drift. As there is no requirement in precision placements of sensors, a sensor-to-segment calibration was taken in prior to obtaining joint axes.

which together compose the gait cycle as shown in Fig. 2. The Bayesian update process is as follows:

$$P(c_n|\omega_t) = \frac{P(\omega_t|c_n)P(c_n|\omega_{t-1})}{P(\omega_t|\omega_{t-1})} \tag{1}$$

where the posterior probability and likelihood at time t are defined by $P(c_n|\omega_t)$ and $P(\omega_t|c_n)$. The prior probability from the previous time $t-1$ is defined by $P(c_n|\omega_{t-1})$. The measurements ω represent the angular rate signals from the IMU sensors attached to the lower limbs of participants.

2) Prior: Uniform prior probabilities for the gait phases are assumed at the initial time $t = 0$, as follows:

$$P(c_n) = P(c_n|\omega_0) = \frac{1}{N} \tag{2}$$

where c_n is the estimated class, ω_0 are the sensor measurements at time $t = 0$ and $N = 2$ is the total number of gait phases (stance and swing phases). For time $t > 0$ the prior distribution is updated by the posterior distribution estimated at time $t-1$, as follows:

$$P(c_n) = P(c_n|\omega_{t-1}) \tag{3}$$

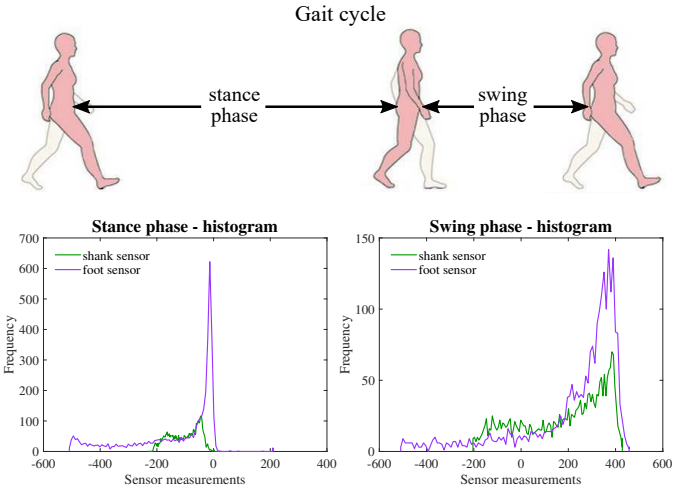

Fig. 2. Gait phases and example of histograms employed for the recognition of stance and swing phases. The histograms are built using data from two IMUs attached to the shank and foot of participants.

3) Measurement model and likelihood estimation: angular rate signals from $S_{\text{sensors}} = 1$ (attached on the shank) are collected during the walking cycle. The collected signals are used to construct the measurement model with a non-parametric approach based on histograms, which evaluate an observation ω_t, and estimate the likelihood of a perceptual class c_n. This process is performed as follows:

$$P_s(b|c_n) = \frac{h_{s,n}(b)}{\sum_{b=1}^{N_{\text{bins}}} h(b)} \tag{4}$$

where $h_{s,n}(b)$ is the sample count in bin b for sensor s over all training data. The histograms are uniformly constructed using $N_{\text{bins}} = 100$ intervals. Fig. 2 shows an example of the histograms built using data from IMUs on the shank and foot. The values are normalised by $\sum_{b=1}^{N_{\text{bins}}} h(b)$ to have probabilities in [0, 1]. The likelihood of the observation ω_t, by evaluating Equation (4) over all sensors, is estimated as follows:

$$\log P(\omega_t|c_n) = \sum_{s=1}^{S_{\text{sensors}}} \frac{\log P_s(b|c_n)}{S_{\text{sensors}}} \tag{5}$$

where $P(\omega_t|c_n)$ is the likelihood of the observation ω_t given a perceptual class c_n. Normalised values in Equation (1) are obtained with the marginal probabilities conditioned from previous sensor observations, as follows:

$$P(\omega_t|\omega_{t-1}) = \sum_{n=1}^{N} P(\omega_t|c_n)P(c_n|\omega_{t-1}) \tag{6}$$

4) Decision making: The Bayesian update process stops once a belief threshold $\beta_{threshold} = [0.0, 0.1, \ldots, 0.99]$ is exceeded. This action enables the decision making process to estimate the gait phase, using the *maximum a posteriori* (MAP) estimate, as follows:

$$\begin{aligned} &\text{if any } P(c_n|\omega_t) > \beta_{threshold} \text{ then} \\ &\hat{c}_n = \arg\max_{c_n} P(c_n|\omega_t) \end{aligned} \tag{7}$$

where $\hat{c}_n$ is the estimated gait phase that tells us whether the human is in stance or swing phase during the walking cycle.

B. Low level - gyroscope and accelerometer integrated ankle angle measurement

The ankle angle is calculated using the complementary filter and sensor-to-segment calibration procedure as shown in Figure 1B. Our method is based on the addition theorem of angular rate and the definition of ankle joint according to the ISB recommendations [29].

1) Identification of the joint axes : The joint is regarded as a hinge joint connecting the two adjacent segments. The proximal segment remains still when the distal segment rotates. The angular rate can be decomposed into components parallel and perpendicular to the joint axis. The perpendicular component can be expressed as:

$$\omega_{\perp} = j \times (\omega \times j) \tag{8}$$

where j represents the joint axis for flexion, ω is angular rate measured from the distal segment.

During the flexion movement, the amplitude of $\omega_{\perp}$ is minimal. The square error of each measurement can be summed into a cost function shown as:

$$C(j) = \sum_{k=1}^{N} \|\omega_{\perp,k}\|^2 \quad = \sum_{k=1}^{N} \|j \times (\omega_k \times j)\|^2 \tag{9}$$

where $\|\cdot\|$ is the Euclidean norm, ω is angular rate, The j has a two parameter expression in spherical coordinates [10]. A vector containing the spherical coordinate parameters can be identified using the cost function C. Note that when j is a unit vector, C can be further simplified: $C(j) = \sum_{k=1}^{N} \|\omega_k \times j\|^2$. We used a MATLAB function *fmincon* (MATLAB 2017b, MathWorks, Natick, USA) to obtain a local minimum of the cost function C.

In our study, inertial sensors are attached to the shank and foot segments as shown in Figure 3A. There are no strict rules about locations of the sensors on the segment and their orientations with respect to the segments. We also assumed that the local sensor axes do not coincide with the joint axes. The joint axes of the shank and foot are determined respectively during the knee flexion/extension and ankle dorsi-/plantarflexion movement.

2) Joint angle calculation: The ankle joint angle is the relative rotation between the shank and foot joint coordinates [29]. If the joint axes are found, the joint coordinates can be created as shown in Figure 3B. The other two axes in the joint coordinates are defined as follows

$$\begin{aligned} x_i &= j_i \times c \\ y_i &= j_i \times x_i \end{aligned} \tag{10}$$

c is an arbitrary unit vector that is not parallel to the joint axis j_i.

Gravity-based acceleration can be expressed by:

$$a^l = D(\hat{q}_{a\omega})g \tag{11}$$

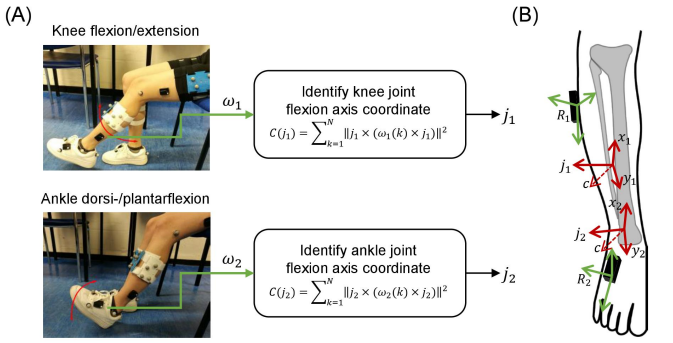

Fig. 3. (A) The procedure of sensor-to-segment calibration. Two sensors were attached to the shank and foot. The subject performed knee flexion/extension and ankle dorsi-/plantarflexion while angular rate data ω_i were recorded. The joint axes j_1 and j_2 were identified using least square cost functions. (B) The joint coordinates were created for the tibia and foot based on the prime joint axes and an arbitrary vector c.

Where $g = (0, 0, 1)^T$ at the global reference frame, D is the direction cosine matrix in the form of (D_1, D_2, D_3) with quaternion $\hat{q}_{a\omega}$ [34]. Eq. 11 can be decomposed as:

$$a^l = D_3(\hat{q}_{a\omega}) = \begin{pmatrix} -q_2 & q_3 & -q_0 & q_1 \\ q_1 & q_0 & q_3 & q_2 \\ q_0 & -q_1 & -q_2 & q_3 \end{pmatrix} \begin{pmatrix} q_0 \\ q_1 \\ q_2 \\ q_3 \end{pmatrix} \tag{12}$$

Its rotation can be represented by the normalised quaternion $\hat{q}_{a\omega}$ that is calculated through acceleration and angular rate data fusion at each time instant as described in Appendix A.

An accelerometer-based joint angle can be approximated using the angle between the projections of local acceleration a_i^l into the joint planes, as follows:

$$\theta_a = \arctan\left(\frac{\|v_1 \times v_2\|}{v_1 \cdot v_2}\right) \tag{13}$$

Where $v_i = a_i^l \cdot [x_i, y_i, 0]$. The joint flexion planes are defined by a pair of axes $x_i, y_i \in \mathbb{R}^3$ from (10).

A gyroscope-based joint angle is calculated by the integration of the difference of the angular rate around the joint axes:

$$\theta_{\omega,t} = \int_0^t (\omega_{1,\tau} \cdot j_1 - \omega_{2,\tau} \cdot j_2) d\tau \tag{14}$$

The gyroscope-based angle is precise on the short time scales but exhibits slow drift over long time measurement. The accelerometer-based angle is not affected by drift, but it is sensitive to measurement noise and may not be reliable at moments when large acceleration change occurs [10] . A complementary filter is used to combine two angles in order to remove the drift in the gyroscope-based angle. An implementation of the complementary filter is given:

$$\theta_{a\omega,t} = \lambda\theta_{a,t} + (1-\lambda)(\theta_{a\omega,t-\triangle t} + \theta_{\omega,t} - \theta_{\omega,t-\triangle t}) \tag{15}$$

C. Real-time protocol

The pseudocode of the gait measurement algorithm in real-time is given as follows in Table I.

TABLE I
PROPOSED GAIT MEASUREMENT ALGORITHMS WITH ACCELERATION AND ANGULAR RATE INPUTS IN REAL-TIME PROGRAM

Initialisation:
t = 0, $f = 148$, $\Delta t = \frac{1}{f}$, $\beta_{threshold} = 0.99$, $\hat{q}_{a\omega,init} = (1,0,0,0)^T$, $\lambda = 0.05$, $d = 0.05$, $d_n = \lfloor d \cdot f \rfloor$, $b_\omega = 0_{1,10}$, $b_{a\omega} = 0_{1,10}$.
Joint axes j_1 and j_2 were determined from the calibration trial.

while no stop commands **and** new acceleration and angular rate data input received
do
High Level

1) **Input**: ω
2) Calculate the likelihood $P(\omega_t|c_n)$
3) Update the posterior $P(c_n|\omega_t) = \frac{P(\omega_t|c_n)P(c_n|\omega_{t-1})}{P(\omega_t|\omega_{t-1})}$
4) **if** $P(c_n|\omega_t) > \beta_{threshold}$ **then**
5) Estimate the gait phase $\hat{c}_n = \arg\max_{c_n} P(c_n|\omega_t)$
6) Go to step 9 to return the estimated class
7) **else** update the prior $P(c_n) = P(c_n|\omega_{t-1})$
8) Go to step 1 to collect more sensor data
9) **Output:** $\hat{c}_n$

Low Level

1) **Input**: $a_1, \omega_1, a_2, \omega_2$
2) $t = t + 1$, $a_i = \frac{a_i}{\|a_i\|}$
3) $q_{i,a\omega}(t) = \left\{ I + \frac{(1-\gamma)\triangle t}{2}[\Omega_i \times] + \gamma \frac{W_{i,a} - I}{2} \right\} \hat{q}_{i,a\omega}(t-1)$
4) $\hat{q}_{i,a\omega}(t) = \frac{q_{i,a\omega}(t)}{\|q_{i,a\omega}(t)\|}$
5) $a_i^l(t) = D_3(\hat{q}_{i,a\omega}(t))$
6) $v_i = a_i^l[x_i, y_i, 0]$, where $x_i = j_i \times c, y_i = j_i \times x_i$
7) $\theta_a = \measuredangle(v_1, v_2)$
8) $\theta_\omega = b_\omega(10) + (\omega_1 \cdot j_1 - \omega_2 \cdot j_2)\Delta t$
9) $\theta_{a\omega} = \lambda\theta_a + (1-\lambda)(b_{a\omega}(10-d_n) + \theta_\omega - b_\omega(10-d_n))$
10) Update buffers $b_{a\omega}$ and b_ω
11) **Output:** $\theta_{a\omega}$

end while

A "zero pose" has to be firstly performed where the measured joint angle is set to zero. The joint angle of the "zero pose" is regarded as the angle offset. Joint angles can be calculated at each time instant by subtracting the angle offset. The offset for the optical reference is also obtained from the "zero pose" trial.

IV. EXPERIMENTS AND RESULTS

A. Experiment Set-up

The study was approved by the ethics committee of the Department of Biomedical Engineering at the University of Strathclyde. Ten participants (six males and four females, age = 26.5 ± 6.2 years) participated. Each participant wore Trigno™ IM sensors (Delsys Inc., USA) attached to the shank and foot of both legs. To validate our real-time gait measurement system, the participant also wore a marker set of Strathclyde functional cluster model [35], Fig 4. A 12 camera Vicon motion capture system (Vicon MX Giganet, Oxford Metrics Ltd., UK) was used as the reference. Marker trajectories were recorded at 100Hz while the accelerations and angular velocities were captured at a frequency of 148 Hz. IMU and stereophotogrammetric data streams were synchronised via an audio signal of START button clicking.

Each participant was instructed to perform knee flexion/extension and ankle dorsi-/plantarflexion in the sensor-to-segment calibration trial, Fig 3. Each movement was repeated ten times. The joint axes were obtained using the method

Fig. 4. Placement of inertial measurement units and optical marker clusters on a subject. The Strathclyde functional cluster model was used to analyse gait phases and kinematics. The IMUs were attached to the thigh, shank and foot without restricting their positions.

described in section III-B1 and stored as a MAT file. A static trial was collected with the participants standing in an anatomical position where the angle offsets for the IMU algorithm and the optical reference were calculated. Subsequently, the participants walked on the treadmill at various speeds (0.5, 1.0 and 1.5 m/s) for 1 minute respectively. The gait measurement system generated the ankle angle and gait phase recognition results simultaneously while the marker trajectories were gathered.

B. Recognition of gait phases

Each gait cycle was divided into two phases: stance and swing. During the stance phase, the foot is in contact with the floor while swing occurs when the foot is in the air. We computed the recognition accuracies from our system assuming the marker trajectories as a reference. The recognition results of gait swing and stance phases are shown by the confusion matrices in Table II. The high-level Bayesian algorithm reached an accuracy of over 95 %, regardless of walking speed for the belief threshold $\beta_{threshold} = 0.99$. This demonstrates that the Bayesian method identifies the stance and swing phases with high accuracy. The effect of treadmill walking speed on the accuracy of gait recognition was also observed in Table II. More errors occurred during the stance phase and the recall decreased with an increased treadmill walking speed. The recognition method achieved the highest accuracy (97.9 % for stance and 96.3 % for swing) at the speed of 1 m/s. The result for swing phase detection was mostly affected when subjects walked at the speed of 1.5 m/s.

Gait events can be further defined during the gait cycle in which heel-strike (HS) is the transition from the swing to stance and toe-off (TO) is the transition from the stance to swing. The time difference between the HS and TO detection and the reference were checked offline as shown in Fig 5. Most of the differences were within the mean $\pm$ 1.96 SD lines, illustrating good agreement between the gait events detection

TABLE II
CONFUSION MATRICES OF GAIT STANCE/SWING PHASE RECOGNITION AT VARIOUS TREADMILL SPEEDS

Speed		Estimated stance	Estimated swing	Precision(%)	Recall (%)	F-measure (%)	Accuracy (%)
0.5 m/s	Actual stance	4421	249	95.8	94.7	95.3	96.2
	Actual swing	192	6668	96.4	97.2	96.8	
1.0 m/s	Actual stance	4687	364	97.9	92.8	95.3	96.5
	Actual swing	100	8074	95.7	98.8	97.2	
1.5 m/s	Actual stance	5088	532	97.0	90.5	93.6	95.1
	Actual swing	156	8392	94.0	98.2	96.1	

and the optical reference. The higher variation in the difference was observed with a speed of 0.5 m/s.

C. Accuracy of ankle angle measurement

The accuracy of the algorithm was evaluated in terms of the root-mean-square error (RMSE), offset and Pearson's correlation coefficients (PCC) between the IMU-based ankle dorsi-/plantarflexion angle measurement and the result from an optical gait analysis system. PCC results in Table III show that the estimated angle using IMU data for the entire dataset had a good agreement with the optical reference (PCC > 0.90).

The resulting ankle angle traces of two different trials for three different speeds are provided in Fig 6A and the deviations between the IMU-based and optical angles are shown in Fig 6B. It shows that the largest errors occur during heel-strike and push-off due to skin tissue artifacts. The proposed IMU-based algorithm achieved an RMSE of less than 3.5°, Table III. The RMSEs of the ankle angle, as well as the offsets, increased as the walking speed increased.

TABLE III
COMPARISON OF THE ANKLE ANGLES BETWEEN IMU-BASED ALGORITHM AND VICON REFERENCE.

Treadmill speed	Offset (deg)	RMSE (deg)	PCC	p
0.5m/s	-0.84 $\pm$ 2.05	2.39 $\pm$ 0.37	0.94 $\pm$ 0.03	0
1.0m/s	4.46 $\pm$ 3.57	2.86 $\pm$ 0.65	0.92 $\pm$ 0.03	0
1.5m/s	7.28 $\pm$ 4.39	3.24 $\pm$ 0.67	0.90 $\pm$ 0.04	0

V. DISCUSSION

This paper proposes a novel gait measurement method that can be used to provide sufficient gait feedback for wearable drop foot assistance devices. A hierarchical model was proposed to obtain simultaneous gait phases recognition and ankle dorsi-/plantarflexion angle. The use of the Bayesian method and sensor-to-segment calibration does not require precise alignment of sensors to the body segments and improves robustness for practical implementation. The proposed method provides good accuracy for both gait phase detection and ankle angle measurement compared to the optical reference.

Most current gait feedback systems focused on precise gait phase recognition [12], [36], [16], [15], [37] while the detected gait event was used as a reliable trigger to start the stimulation. Seel et al. [1] measured foot pitch angle and four gait phases by placing a 6D IMU on the foot, and based on which an iterative learning control scheme was developed. Results showed that the closed-loop approach would facilitate the adaptation from patient to patient. A multilayer architecture is recognised to be essential for intelligent systems to perform robust data processing, perception, and action at different levels of abstraction [11]. Our work could be extended to include the high and low-level process of robotic control in real-time.

The performance of the Bayesian method was analysed with the recognition of gait phases. The gait cycle was segmented into stance and swing phases, which were successfully recognised with an accuracy of 97.9% and 96.3%, respectively at the speed of 1 m/s. The performance of gait recognition was affected by the walking speed as shown in Table II, which may be related to subjects' walking speed in the training dataset and the overground walking experimental set-up. Despite this reduction in accuracy, the recognition method is robust considering that the algorithm was not re-trained with data from new subjects. Previous works, using a variety of machine learning algorithms and sensor sets have been able to achieve accuracies of 91%, 99% and 100% [15], [13], [37], [18]. However, they present limitations such as fixed sampling window size, a large number of sensors, black box models and the need for algorithm re-training for new subjects. Delay time in real-time systems with sophisticated machine learning algorithms was over 35ms [36], [38], [37]. A simple state machine learning method achieved a shorter decision delay time of 23 ms [12]. Our Bayesian formulation with a sequential analysis method obtained a response time of less than 20ms (Figure 5). The method was able to react fast with high accuracy to distinguish gait phases with the use of a single IMU sensor attached to the lateral side of the shank. The detection of additional gait phases will be considered in future studies for active ankle-foot assistance.

In this study, a sensor-to-segment calibration procedure was proposed to determine the joint axes allowing the determination of joint angles without the need for specific IMU alignment. Favre et al. [31] firstly proposed a calibration procedure for IMUs to describe the knee joint according to the ISB recommendations. The study showed that accuracies of joint axes localisation are sensitive to the execution of the calibration. Seel et al. [10] proposed a method using acceleration and angular rate to find local joint axes and position for the joints. Our proposed method employs only accelerometers and gyroscopes readings so that it is more suitable for the use of indoor application. It is simple and efficient without requiring local positions to the joint for calculating the accelerometer-based angle. We define the ankle dorsi-/plantarflexion angle as the angle between the shank and foot along the flexion axis. However, we shall note that considering the ankle as a hinge joint is an assumption. Although dorsi-/plantarflexion is

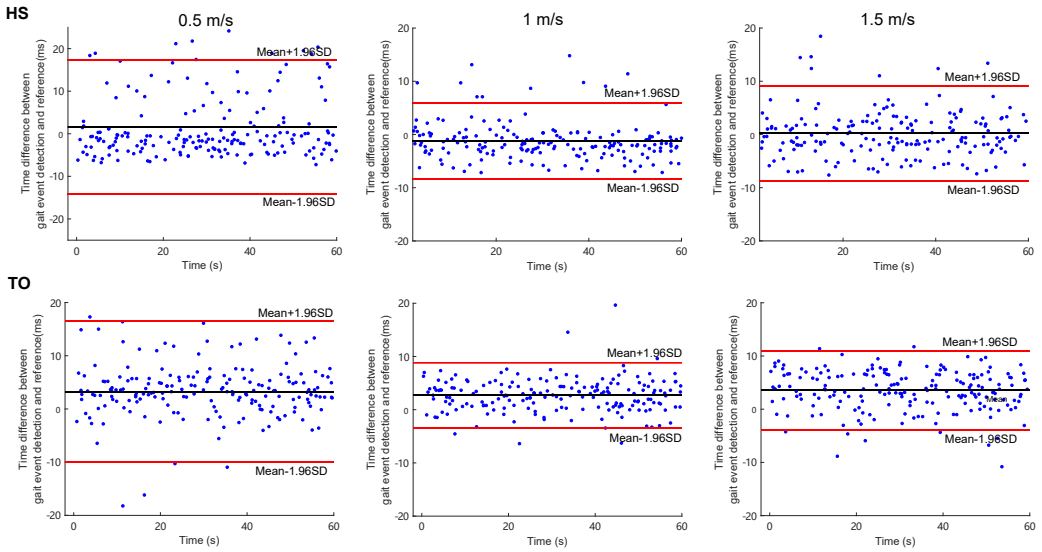

Fig. 5. The time difference between the heel-strike (HS) and toe-off (TO) gait event detection and the reference from the optical system at various speeds (0.5m/s, 1.0m/s, 1.5m/s).

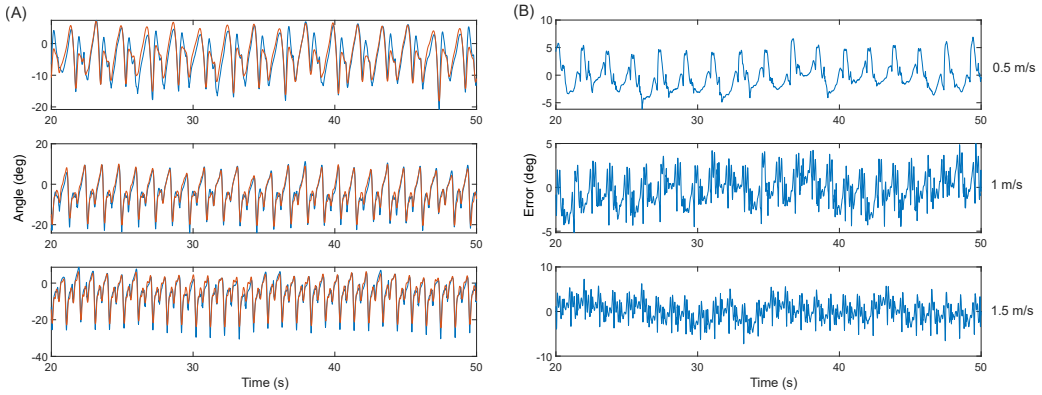

Fig. 6. (A) Comparison of ankle angle estimates using IMU data (red) and reference optical system (blue) for Subject 1 at three different speeds (0.5 m/s, 1.0 m/s and 1.5 m/s). (B) Ankle angle estimation error from IMU data and reference for Subject 1 at three different speeds.

the major degree of freedom, the joint is not constrained to rotate around one axis, which leads to a 3D ankle joint angle measurement in some scenarios. The proposed algorithm can be easily extended for 3D angle measurement on the ankle joint.

The method obtained PPCs in the range from 0.90 to 0.94 and RMSEs within 3.5 degrees for the ankle angle at three different speeds when compared to the optical reference. The results are comparable with those presented in [39], [40] where the joint angle remained under an acceptable level of 5 degrees RMSE. Results in Table III showed that the quality of angle measurement decreases while the treadmill walking speed increases. This is consistent with results in previous studies (reviewed in [41]). Skin tissue artefact (STA) is a major source of RMSE by applying additional noise to the body-worn sensors [42]. The increase of STA amplitude while the treadmill speed incremented would result in an increase of the RMSE and PCC. Compared to the knee angle, the ankle angle measurement is more affected by treadmill speed variation [43]. The offset may come from linear displacement of the stance foot contacting the treadmill.

The method was only tested on able-bodied participants. The algorithm validation on patients with drop foot should be considered. Future research will consider the extension of the dataset, including participants affected by neurological diseases, such as spinal cord injured and stroke.

VI. CONCLUSION

This work presented a novel gait measurement method for providing sensory feedback for the control of drop foot correction. The method used acceleration and angular rate from wearable IMUs attached to the shank and foot. A two-layer model was developed to recognise the stance and swing phases and measure the ankle angle simultaneously. The online performance of the method was investigated. The recognition of gait phases and ankle angle were compared to optical references when the participants walked on a treadmill with three different speeds. The results demonstrated that our method offered an efficient approach for applications in the adaptive control of drop foot assistance.

APPENDIX A
QUATERNION ESTIMATION WITH ACCELEROMETER AND GYROSCOPE SENSOR FUSION

The 3D angular rate ω and 3D acceleration a can be defined by

$$\begin{aligned} \omega &= (\omega_x, \omega_y, \omega_z)^T \\ a &= (a_x, a_y, a_z)^T \end{aligned} \tag{16}$$

The relationship between quaternion and the angular rate is usually described as a differential equation

$$\begin{aligned} \dot{q}_\omega(t) &= \frac{1}{2}[\Omega\times]q_\omega(t-1) \\ &= \frac{1}{2}\begin{bmatrix} 0 & -\omega_x & -\omega_y & -\omega_z \\ \omega_x & 0 & \omega_z & -\omega_y \\ \omega_y & -\omega_z & 0 & \omega_x \\ \omega_z & \omega_y & -\omega_x & 0 \end{bmatrix} q_\omega(t-1) \end{aligned} \tag{17}$$

The quaternion is therefore calculated through gyroscope integration at the time t.

$$q_\omega(t) = q_\omega(t-1) + \dot{q}_\omega(t)\triangle t \tag{18}$$

A first-order complimentary filter model is used, which introduces the accelerometer to compensate for the error of the angular rate.

$$\dot{q}_{a\omega}(t) = (1-\gamma)\dot{q}_\omega(t) + \gamma\dot{q}_a(t) \tag{19}$$

Where γ is set to 0.05, quaternion incrementation from accelerometer is defined as the following equation. Its calculation is well explained in [34].

$$\begin{aligned} \triangle q_a &= \frac{W_a - I}{2} q_0 \\ &= \frac{1}{2}\begin{bmatrix} a_z - 1 & a_y & -a_x & 0 \\ a_y & -a_z - 1 & 0 & a_x \\ -a_x & 0 & -a_z - 1 & a_y \\ 0 & a_x & a_y & a_z - 1 \end{bmatrix} q_0 \end{aligned} \tag{20}$$

The estimation of quaternion calculated through gyroscope and accelerometer fusion can be described as

$$q_{a\omega}(t) = q_{a\omega}(t-1) + \dot{q}_{a\omega}(t)\triangle t \tag{21}$$

This equation can be further expressed by substituting Eq 19, 17 and 20.

$$\begin{aligned} q_{a\omega}(t) &= \hat{q}_{a\omega}(t-1) + [(1-\gamma)\dot{q}_\omega(t) + \gamma\dot{q}_a(t)]\triangle t \\ &= \hat{q}_{a\omega}(t-1) + \frac{1-\gamma}{2}[\Omega\times]\hat{q}_{a\omega}(t-1) + \gamma\triangle q_a \\ &= \left\{\frac{(1-\gamma)\triangle t}{2}[\Omega\times] + I\right\}\hat{q}_{a\omega}(t-1) + \gamma\frac{W_a - I}{2}\hat{q}_{a\omega}(t-1) \\ &= \left\{I + \frac{(1-\gamma)\triangle t}{2}[\Omega\times] + \gamma\frac{W_a - I}{2}\right\}\hat{q}_{a\omega}(t-1) \end{aligned} \tag{22}$$

Note that a normalisation step is taken after each update.

REFERENCES

[1] T. Seel, C. Werner, J. Raisch, and T. Schauer, "Iterative learning control of a drop foot neuroprosthesis — generating physiological foot motion in paretic gait by automatic feedback control," *Control Engineering Practice*, vol. 48, pp. 87–97, 2016.

[2] L. R. Sheffler and J. Chae, "Neuromuscular electrical stimulation in neurorehabilitation," *Muscle & Nerve*, vol. 35, no. 5, pp. 562–590, 2007.

[3] E. Ambrosini, S. Ferrante, G. Ferrigno, F. Molteni, and A. Pedrocchi, "Cycling induced by electrical stimulation improves muscle activation and symmetry during pedaling in hemiparetic patients," *IEEE Transactions on Neural Systems and Rehabilitation Engineering*, vol. 20, no. 3, pp. 320–330, May 2012.

[4] Y.-L. Park, B. rong Chen, N. O. Pérez-Arancibia, D. Young, L. Stirling, R. J. Wood, E. C. Goldfield, and R. Nagpal, "Design and control of a bio-inspired soft wearable robotic device for ankle–foot rehabilitation," *Bioinspiration & Biomimetics*, vol. 9, no. 1, p. 016007, jan 2014.

[5] F. Patané, S. Rossi, F. Del Sette, J. Taborri, and P. Cappa, "Wake-up exoskeleton to assist children with cerebral palsy: Design and preliminary evaluation in level walking," *IEEE Transactions on Neural Systems and Rehabilitation Engineering*, vol. 25, no. 7, pp. 906–916, July 2017.

[6] M. Zhang, J. Cao, S. Q. Xie, G. Zhu, X. Zeng, X. Huang, and Q. Xu, "A preliminary study on robot-assisted ankle rehabilitation for the treatment of drop foot," *Journal of Intelligent & Robotic Systems*, vol. 91, no. 2, pp. 207–215, Aug 2018.

[7] G. M. Lyons, T. Sinkjaer, J. H. Burridge, and D. J. Wilcox, "A review of portable fes-based neural orthoses for the correction of drop foot," *IEEE transactions on neural systems and rehabilitation engineering : a publication of the IEEE Engineering in Medicine and Biology Society*, vol. 10, no. 4, p. 260—279, December 2002.

[8] I. P. I. Pappas, M. R. Popovic, T. Keller, V. Dietz, and M. Morari, "A reliable gait phase detection system," *IEEE Transactions on Neural Systems and Rehabilitation Engineering*, vol. 9, no. 2, pp. 113–125, June 2001.

[9] A. Mansfield and G. M. Lyons, "The use of accelerometry to detect heel contact events for use as a sensor in fes assisted walking," *Medical Engineering & Physics*, vol. 25, no. 10, pp. 879 – 885, 2003.

[10] T. Seel, J. Raisch, and T. Schauer, "Imu-based joint angle measurement for gait analysis," *Sensors*, vol. 14, no. 4, pp. 6891–6909, 2014.

[11] U. Martinez-Hernandez, I. Mahmood, and A. A. Dehghani-Sanij, "Simultaneous bayesian recognition of locomotion and gait phases with wearable sensors," *IEEE Sensors Journal*, vol. 18, no. 3, pp. 1282–1290, Feb 2018.

[12] J. Rueterbories, E. G. Spaich, and O. K. Andersen, "Gait event detection for use in fes rehabilitation by radial and tangential foot accelerations," *Medical Engineering & Physics*, vol. 36, no. 4, pp. 502–508, 2014.

[13] N. C. Bejarano, E. Ambrosini, A. Pedrocchi, G. Ferrigno, M. Monticone, and S. Ferrante, "A novel adaptive, real-time algorithm to detect gait events from wearable sensors," *IEEE Transactions on Neural Systems and Rehabilitation Engineering*, vol. 23, no. 3, pp. 413–422, May 2015.

[14] R. Kamnik and T. Bajd, "Standing-up robot: an assistive rehabilitative device for training and assessment," *Journal of Medical Engineering & Technology*, vol. 28, no. 2, pp. 74–80, 2004.

[15] R. Williamson and B. J. Andrews, "Gait event detection for fes using accelerometers and supervised machine learning," *IEEE Transactions on Rehabilitation Engineering*, vol. 8, no. 3, pp. 312–319, Sep. 2000.

[16] M. S. H. Aung, S. B. Thies, L. P. J. Kenney, D. Howard, R. W. Selles, A. H. Findlow, and J. Y. Goulermas, "Automated detection of instantaneous gait events using time frequency analysis and manifold embedding," *IEEE Transactions on Neural Systems and Rehabilitation Engineering*, vol. 21, no. 6, pp. 908–916, Nov 2013.

[17] J. Taborri, S. Rossi, E. Palermo, F. Patanè, and P. Cappa, "A novel hmm distributed classifier for the detection of gait phases by means of a wearable inertial sensor network," *Sensors*, vol. 14, no. 9, pp. 16 212–16 234, 2014.

[18] M. Yuwono, S. W. Su, Y. Guo, B. D. Moulton, and H. T. Nguyen, "Unsupervised nonparametric method for gait analysis using a waist-worn inertial sensor," *Applied Soft Computing*, vol. 14, pp. 72 – 80, 2014, special issue on hybrid intelligent methods for health technologies.

[19] J. Morris, "Accelerometry—a technique for the measurement of human body movements," *Journal of Biomechanics*, vol. 6, no. 6, pp. 729 – 736, 1973.

[20] A. M. Sabatini, "Quaternion based attitude estimation algorithm applied to signals from body-mounted gyroscopes," *Electronics Letters*, vol. 40, no. 10, pp. 584–586, May 2004.

[21] K. Tong and M. H. Granat, "A practical gait analysis system using gyroscopes," *Medical Engineering & Physics*, vol. 21, no. 2, pp. 87 – 94, 1999.

[22] H. Saito, T. Watanabe, and A. Arifin, "Ankle and knee joint angle measurements during gait with wearable sensor system for rehabilitation," in *World Congress on Medical Physics and Biomedical Engineering, September 7 - 12, 2009, Munich, Germany*, O. Dössel and W. C. Schlegel, Eds. Berlin, Heidelberg: Springer Berlin Heidelberg, 2009, pp. 506–509.

[23] F. Alonge, E. Cucco, F. D'Ippolito, and A. Pulizzotto, "The use of accelerometers and gyroscopes to estimate hip and knee angles on gait analysis," *Sensors*, vol. 14, no. 5, pp. 8430–8446, 2014.

[24] H. Dejnabadi, B. M. Jolles, E. Casanova, P. Fua, and K. Aminian, "Estimation and visualization of sagittal kinematics of lower limbs orientation using body-fixed sensors," *Ieee Transactions on Biomedical Engineering*, vol. 53, no. 7, pp. 1385–1393, 2006.

[25] E. Bergamini, G. Ligorio, A. Summa, G. Vannozzi, A. Cappozzo, and A. M. Sabatini, "Estimating orientation using magnetic and inertial sensors and different sensor fusion approaches: Accuracy assessment in manual and locomotion tasks," *Sensors*, vol. 14, no. 10, pp. 18 625–18 649, 2014.

[26] W. Teufl, M. Miezal, B. Taetz, M. Fröhlich, and G. Bleser, "Validity, test-retest reliability and long-term stability of magnetometer free inertial sensor based 3d joint kinematics," *Sensors*, vol. 18, no. 7, 2018.

[27] D. Laidig, T. Schauer, and T. Seel, "Exploiting kinematic constraints to compensate magnetic disturbances when calculating joint angles of approximate hinge joints from orientation estimates of inertial sensors," in *2017 International Conference on Rehabilitation Robotics (ICORR)*, July 2017, pp. 971–976.

[28] J. Favre, B. M. Jolles, O. Siegrist, and K. Aminian, "Quaternion-based fusion of gyroscopes and accelerometers to improve 3d angle measurement," *Electronics Letters*, vol. 42, no. 11, pp. 612–614, May 2006.

[29] G. Wu, S. Siegler, P. Allard, C. Kirtley, A. Leardini, D. Rosenbaum, M. Whittle, D. D. D'Lima, L. Cristofolini, H. Witte, O. Schmid, and I. Stokes, "Isb recommendation on definitions of joint coordinate system of various joints for the reporting of human joint motion—part i: ankle, hip, and spine," *Journal of Biomechanics*, vol. 35, no. 4, pp. 543 – 548, 2002.

[30] K. Liu, T. Liu, K. Shibata, and Y. Inoue, "Ambulatory measurement and analysis of the lower limb 3d posture using wearable sensor system," in *2009 International Conference on Mechatronics and Automation*, Aug 2009, pp. 3065–3069.

[31] J. Favre, R. Aissaoui, B. Jolles, J. de Guise, and K. Aminian, "Functional calibration procedure for 3d knee joint angle description using inertial sensors," *Journal of Biomechanics*, vol. 42, no. 14, pp. 2330 – 2335, 2009.

[32] L. Daniel, M. Philipp, and S. Thomas, "Automatic anatomical calibration for imu-based elbow angle measurement in disturbed magnetic fields," *Current Directions in Biomedical Engineering*, vol. 3, no. 2, pp. 167–170, 2017, 2.

[33] T. McGrath, R. Fineman, and L. Stirling, "An auto-calibrating knee flexion-extension axis estimator using principal component analysis with inertial sensors," *Sensors*, vol. 18, no. 6, 2018. [Online]. Available: https://www.mdpi.com/1424-8220/18/6/1882

[34] J. Wu, Z. Zhou, J. Chen, H. Fourati, and R. Li, "Fast complementary filter for attitude estimation using low-cost marg sensors," *IEEE Sensors Journal*, vol. 16, no. 18, pp. 6997–7007, Sept 2016.

[35] L. J. Millar, L. Meng, and P. J. Rowe, "Routine clinical motion analysis: comparison of a bespoke real-time protocol to current clinical methods," *Computer Methods in Biomechanics and Biomedical Engineering*, vol. 0, no. 0, pp. 1–10, 2018.

[36] R. C. González, A. M. López, J. Rodriguez-Uría, D. Álvarez, and J. C. Alvarez, "Real-time gait event detection for normal subjects from lower trunk accelerations," *Gait & Posture*, vol. 31, no. 3, pp. 322 – 325, 2010.

[37] A. Mannini, V. Genovese, and A. M. Sabatini, "Online decoding of hidden markov models for gait event detection using foot-mounted gyroscopes," *IEEE Journal of Biomedical and Health Informatics*, vol. 18, no. 4, pp. 1122–1130, July 2014.

[38] A. Mannini and A. M. Sabatini, "Gait phase detection and discrimination between walking-jogging activities using hidden markov models applied to foot motion data from a gyroscope," *Gait & posture*, vol. 36, no. 4, p. 657—661, September 2012.

[39] T. Seel, D. Graurock, and T. Schauer, "Realtime assessment of foot orientation by accelerometers and gyroscopes," *Current Directions in Biomedical Engineering*, vol. 1, no. 1, p. 466–469, 2015. [Online]. Available: https://www.degruyter.com/view/j/cdbme.2015.1.issue-1/cdbme-2015-0112/cdbme-2015-0112.xml

[40] X. Robert-Lachaine, H. Mecheri, C. Larue, and A. Plamondon, "Validation of inertial measurement units with an optoelectronic system for whole-body motion analysis," *Medical & Biological Engineering & Computing*, vol. 55, no. 4, pp. 609–619, Apr 2017.

[41] I. Poitras, F. Dupuis, M. Bielmann, A. Campeau-Lecours, C. Mercier, L. J. Bouyer, and J.-S. Roy, "Validity and reliability of wearable sensors for joint angle estimation: A systematic review," *Sensors*, vol. 19, no. 7, 2019. [Online]. Available: https://www.mdpi.com/1424-8220/19/7/1555

[42] T. Bonci, V. Camomilla, R. Dumas, L. Chèze, and A. Cappozzo, "A soft tissue artefact model driven by proximal and distal joint kinematics," *Journal of Biomechanics*, vol. 47, no. 10, pp. 2354 – 2361, 2014.

[43] M. D. Djurić-Jovičić, N. S. Jovičić, and D. B. Popovcić, "Kinematics of gait: New method for angle estimation based on accelerometers," *Sensors*, vol. 11, no. 11, pp. 10 571–10 585, 2011.

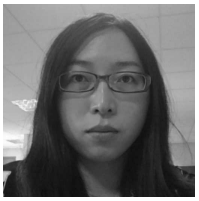

Lin Meng received the PhD degree from the division of Biomedical Engineering, University of Glasgow, Glasgow, U.K., in 2016. She is currently an Associate professor at Tianjin International Joint Research Center for Neural Engineering, Academy of Medical Engineering and Translational Medicine, Tianjin University, Tianjin, China. Her research interests include motion analysis, wearable sensing technologies, and assistive robotics.

Uriel Martinez-Hernandez received the PhD degree from the Department of Automatic Control and Systems Engineering, University of Sheffield, Sheffield, U.K., in 2014. He is currently a Lecturer (Assistant Professor) in Robotics at the Department of Electronics and Electrical Engineering, University of Bath, Bath, U.K. His research interests include touch and vision sensing, wearable assistive robotics, active perception and machine learning for autonomous robots.

Craig Childs received the PhD degree from the University of Aalborg, Denmark. He is currently a Research Fellow at the Biomedical Engineering Department at the University of Strathclyde, Glasgow, UK. He is a Clinical Scientist registered with the HCPC. His research interests include motion analysis, gait stability, virtual reality feedback, wearable sensors and accessibility.

Abbas A. Dehghani-Sanij received the PhD degree from the University of Leeds, Leeds, U.K. He is currently Professor of Bio-Mechatronics and Medical Robotics in the School of Mechanical Engineering at the University of Leeds, Leeds, U.K. His research interests include robotics, biomechatronics, intelligent control, sensors and actuators for the development of intelligent systems/devices. He has published more than 90 journal and conference papers.

Arjan Buis received the PhD degree from the University of Strathclyde. He is currently an Associate professor at the Biomedical Engineering department at the University of Strathclyde, Glasgow, UK. He is a biomedical engineer and Sr, prosthetist & Orthotist. His research interests include the body device interface, wearable sensing technologies, assistive robotics. He has published over 100 journal and conference papers.